Hindawi Publishing Corporation
Journal of Nanomaterials
Volume 2015, Article ID 412515, 5 pages
http://dx.doi.org/10.1155/2015/412515

Research Article

3D Flower-Like Hierarchitectures Constructed by SnS/SnS_2 Heterostructure Nanosheets for High-Performance Anode Material in Lithium-Ion Batteries

Zhiguo Wu, Fengyi Wang, Shiyong Zuo, Shuankui Li, Baisong Geng, Renfu Zhuo, and Pengxun Yan

School of Physical Science and Technology, Lanzhou University, Lanzhou, Gansu 730000, China

Correspondence should be addressed to Zhiguo Wu; zgwu@lzu.edu.cn

Received 10 July 2015; Revised 7 October 2015; Accepted 20 October 2015

Academic Editor: Qiquan Qiao

Sn chalcogenides, including SnS, Sn_2S_3, and SnS_2, have been extensively studied as anode materials for lithium batteries. In order to obtain one kind of high capacity, long cycle life lithium batteries anode materials, three-dimensional (3D) flower-like hierarchitectures constructed by SnS/SnS_2 heterostructure nanosheets with thickness of ~20 nm have been synthesized via a simple one-pot solvothermal method. The obtained samples exhibit excellent electrochemical performance as anode for Li-ion batteries (LIBs), which deliver a first discharge capacity of 1277 $mAhg^{-1}$ and remain a reversible capacity up to 500 $mAhg^{-1}$ after 50 cycles at a current of 100 mAg^{-1}.

1. Introduction

Owing to the high theoretical gravimetric lithium storage capacity, Sn chalcogenides, including SnS, Sn_2S_3, and SnS_2, have been extensively studied as anode materials for lithium-ion batteries [1–5]. To the tin-based materials, the large volume changing, during the lithiation/delithiation process, often causes a drastic pulverization problem [6]. It is an effective method to produce a nanometer-sized frame, which cannot only shorten the pathway lengths of lithium-ions but also compensate the volume change due to their large surface-volume ratio, by morphology controlling [7]. Since then, tremendous efforts have been made to synthesize SnS_2 and SnS nano/microstructures and remarkable progress has been achieved [8, 9]. However, there are very few reports on the synthesis of well-defined 3D nanostructures constructed by SnS/SnS_2 heterogeneous nanosheets and their electrochemical study in lithium-ion battery fields.

Herein, we demonstrate a facile, one-pot solvothermal route for the preparation of well-defined 3D nanostructures constructed by SnS/SnS_2 heterogeneous nanosheets. The nanosheet comprises a single-crystal SnS nanosheet base and a thin layer SnS_2 coat on its surfaces. Compared with the previous two-step growth method for heterostructures, this one-step hydrothermal strategy is more convenient and effective. Furthermore, electrochemical measurements show that the nanoflowers will be a promising anode candidate for rechargeable lithium-ion batteries.

2. Experimental Details

Tin (II) chloride dehydrate ($SnCl_2{\cdot}2H_2O$, 98%), citric acid, thiourea (CH_4N_2S), and ethylene glycol (EG) were analytical grade and used without further purification. In a typical growth, $SnCl_2{\cdot}2H_2O$ (1 mmol), CH_4N_2S (3 mmol), and citric acid (1 mmol) were dissolved in 30 mL ethylene glycol under vigorous magnetic stirring to form an even solution. The homogeneous was transferred to a 40 mL Teflon-lined autoclave. And then the autoclave was kept in a muffle furnace at 190°C for 18 h. Cooling down to room temperature naturally, the black solid product was collected by centrifugation and washed three times with deionized water and ethyl alcohol, respectively, and dried at 80°C. The structure and morphology of the 3D flower-like hierarchitectures have been characterized by X-ray diffraction (XRD), scanning electron

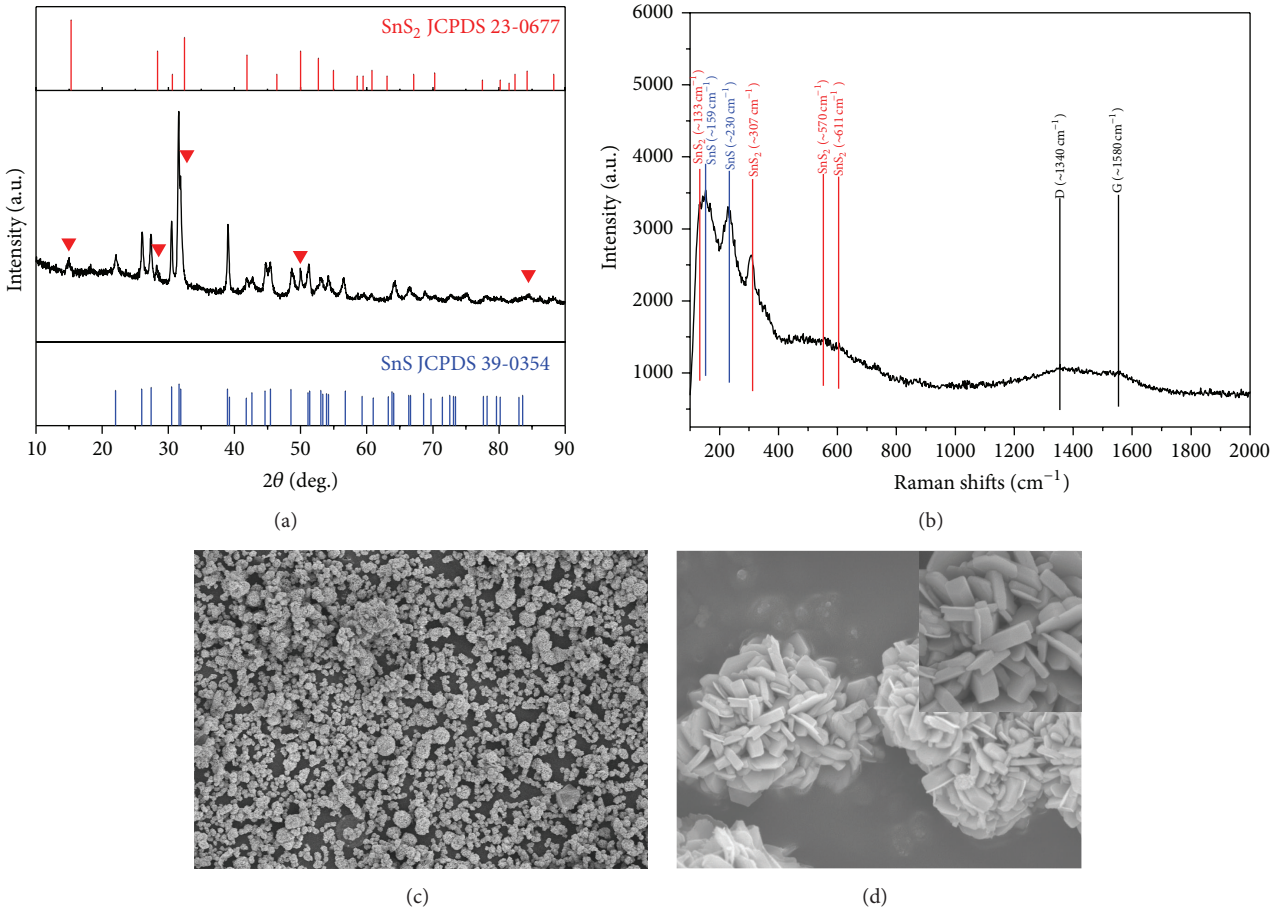

Figure 1: (a) XRD pattern and (b) Raman spectrum of the as-synthesized sample. And the reference patterns are the standard Hexagonal (JCPDS 23-0677) and the standard Herzenbergite (JCPDS 39-0354). (c) and (d) FESEM images with different magnifications of the as-synthesized sample (the insert is the high magnification image).

microscopy (SEM), and transmission electron microscopy (TEM).

The batteries were assembled in a glovebox which was filled by high purity argon gas. The anodes were composed of obtained products, carbon black, and poly(vinylidene fluoride) (PVDF), with a weight ratio of 85 : 10 : 5. The typical loading density on a Cu foil was ~1.5 mg cm^{-2}. A Li foil was used as the cathode. $LiPF_6$ (1 M) in ethylene carbonate (EC)/diethyl carbonate (DEC) (1 : 1 w/w) was used as the electrolyte. The charge/discharge tests were performed using a multichannel battery workstation (Lande Co., China).

3. Results and Discussion

The crystallinity and phase of the products were examined by powder XRD (Figure 1(a)). It can be seen that the sample shows an orthorhombic phase structure of SnS (JCPDS: 39-0354) and a hexagonal structure of SnS_2 (JCPDS: 23-0677). No additional peaks other than SnS or SnS_2 were observed. Figure 1(b) shows the Raman spectrum of as-prepared sample. Raman-active vibrational modes associated with the orthorhombic phase SnS with peak positions around 159 cm^{-1} and 230 cm^{-1} were observed in the sample. The Raman peaks at 133 cm^{-1}, 307 cm^{-1}, 570 cm^{-1}, and 611 cm^{-1} in sample closely confirm the reported spectrum of SnS_2 crystal of the 2H polytype structure [10, 11]. The Raman signatures of G band (~1580 cm^{-1}) and a D band (~1340 cm^{-1}) confirm the existence of amorphous carbon [12].

The morphologies of as-prepared samples were illuminated by electron microscopy images, as shown in Figures 1(c) and 1(d). The full view SEM image (Figure 1(c)) affirms the large-scale production of the united flower-like structures with an average diameter of 5 μm. The detailed morphology of the flower-like nanostructures is shown in Figure 1(d), which reveals that the entire structure of the architecture is built from 2D petal-like building units with smooth surfaces. The nanopetals connected to each other through the centre to form 3D flower-like structures. The internal cross-linked structure of the nanopetals would effectively prevent lamella aggregation and maintains the long-standing existence of the hierarchitecture. Interestingly, each of the petal-like building units is constructed by a thick sheet about 100 nm and a thin sheet about 10 nm with distinct boundary, as shown in the inset of Figure 1(d).

The TEM images further confirm the formation of regular flower-like hierarchitectures (Figure 2(a)). High-resolution

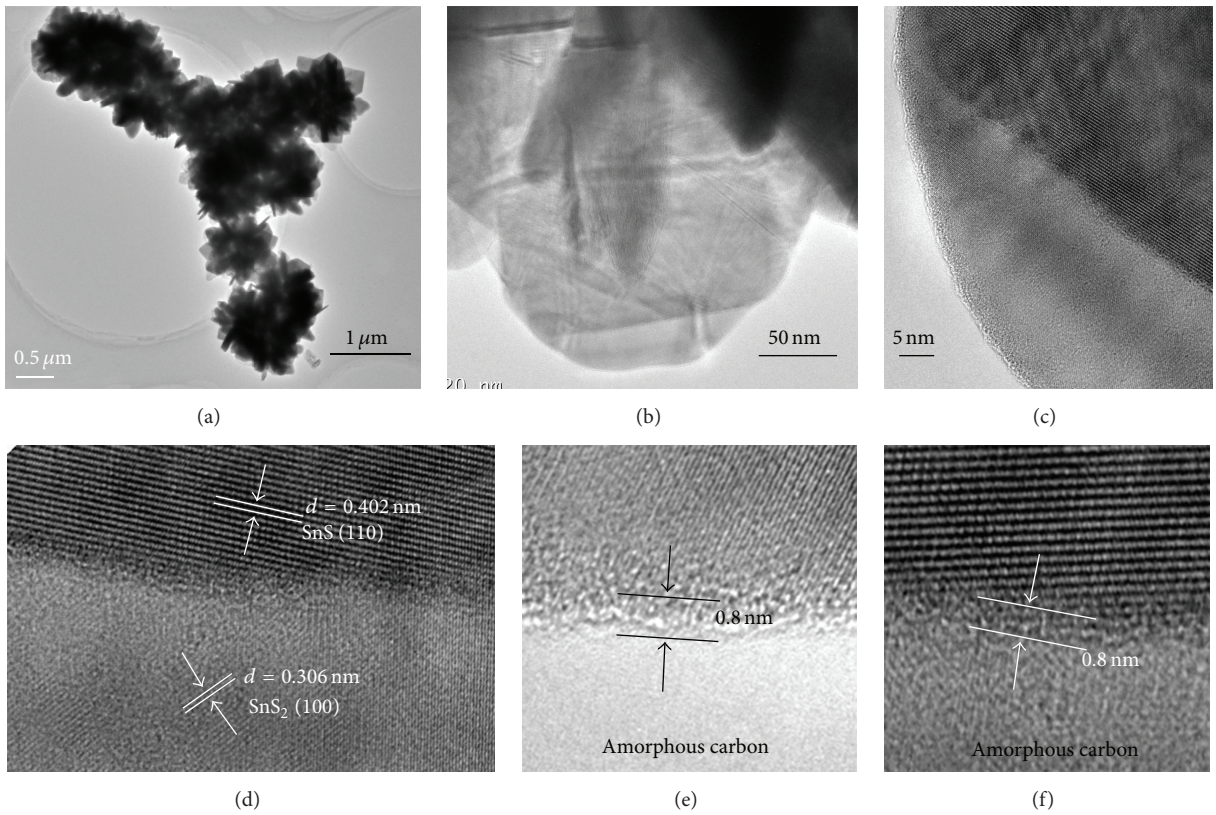

Figure 2: TEM and HRTEM images of the as-synthesized sample. (a) The TEM image of the SnS/SnS_2 nanoflower. (b) and (c) The HRTEM image of individual SnS/SnS_2 nanosheet. (d) The boundaries between SnS and SnS_2. (e) and (f) HRTEM images of the carbon layer on the surface.

TEM (HRTEM) images showed the lattice-resolved fringes in both the two layer nanosheets, indicating the single crystalline nature of both portions (Figure 2(c)). The lattice spacing in the thick nanosheet base was 0.402 nm, corresponding to the (110) planes of SnS. The lattice spacing in the thin nanosheet was 0.306 nm, in good accord with d values of the (100) planes in a hexagonal SnS_2. There are clear boundaries observed between the two phases. It is should be pointed out that there is a 0.8 nm amorphous carbon layer found over the entire surface, which has been confirmed by Raman signatures. Citrate anions play key roles in the formation of these amorphous carbon layers on the SnS nanosheets since Co_3O_4-C hybrid core-shell and hollow spheres have been reported in similar process [13].

We studied the electrochemical properties of as-prepared sample using galvanostatic discharge and cyclic voltammetry measurements. According to previous reports, the lithium intercalation and conversion reactions based on the formation of metallic Sn and subsequent generation of a Li-Sn alloy [14–16] are as follows:

$$SnS + xLi^+ + xe^- \longrightarrow Li_2S + Sn \quad (1)$$

$$SnS_2 + xLi^+ + xe^- \longrightarrow Li_2S + Sn \quad (2)$$

$$Sn + xLi^+ + xe^- \longleftrightarrow Li_xSn \quad (0 \le x \le 4.4) \quad (3)$$

Figure 3(a) shows the cyclic voltammetric (C-V) curves which were tested at a scan rate of 0.2 mVs^{-1} over a voltage range from 0.02 to 1.3 V. Three small reduction peaks at 0.1, 0.27, and 0.56 V are assigned to the lithium insertion into anode material to form Li_xSn alloy. The cathodic peak at 1.12 V, observed during the first sweep, was assigned to the decomposition of the SnS and SnS_2 into metallic tin and Li_2S (1) and (2) and the formation of solid electrolyte interface (SEI), which should be the direct reason for the first irreversible capacity loss. Oxidation peaks at 0.56 V and 0.67 V correspond to the delithiation reaction of Li_xSn alloy. Figure 3(b) shows the voltage-capacity profile of the SnS/SnS_2 nanoflower electrode a current density of 100 mAg^{-1}, with the voltage from 0.02 to 2.5 V. From the first cycle voltage-capacity profile, the initial discharge capacity is 1278 $mAhg^{-1}$. There is one plateau at about 1.12 V during the first discharge process and it disappears after the first cycle, which can be ascribed to the SnS and SnS_2 converted into Sn and the formation of Li_2S. The existence of the plateau at 1.12 V is the major reason for the more large discharge capacity than the next cycles [17].

In Figure 4(a) the electrochemical cycling tests of the sample were performed over the potential range of 0.02 V to 1.3 V at a current density of 100 mAg^{-1}. The discharge-charge profiles revealed an initial discharge capacity of 1277 $mAhg^{-1}$ and the initial recharge capacity is about 613 $mAhg^{-1}$,

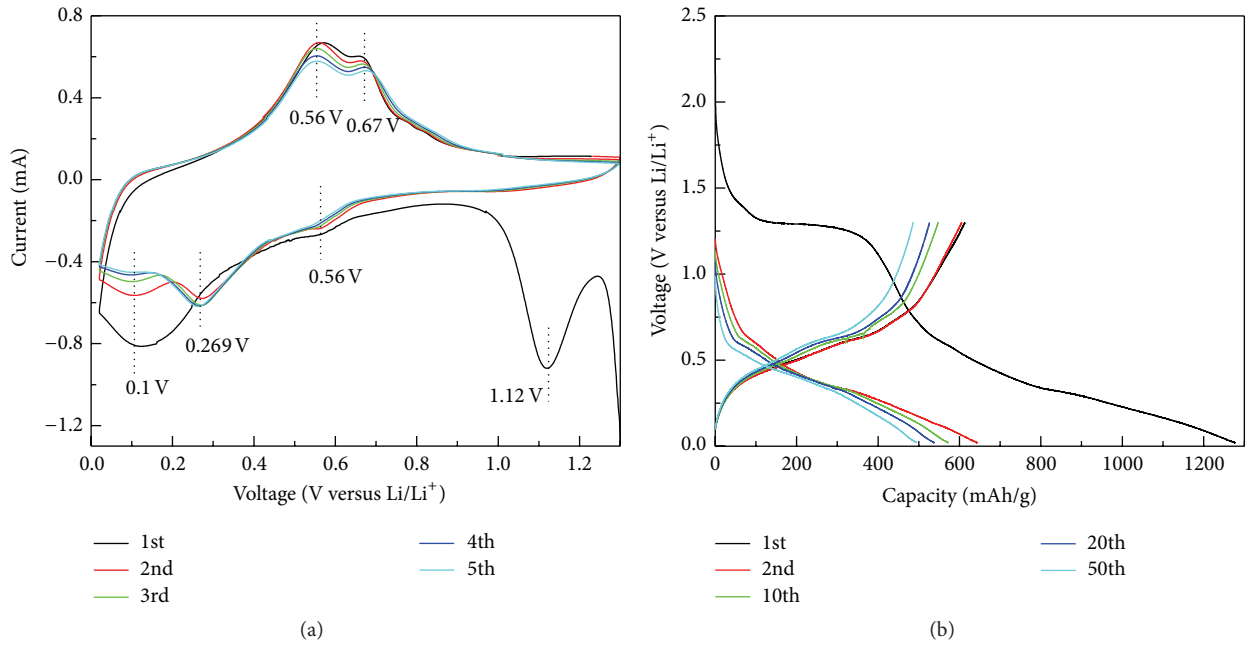

FIGURE 3: (a) Cycle voltammogram of the SnS/SnS_2 nanoflower electrode at a scan rate of 0.2 mVs^{-1}. (b) Voltage-capacity profile of the SnS/SnS_2 nanoflower electrode at a current density of 100 mAg^{-1}.

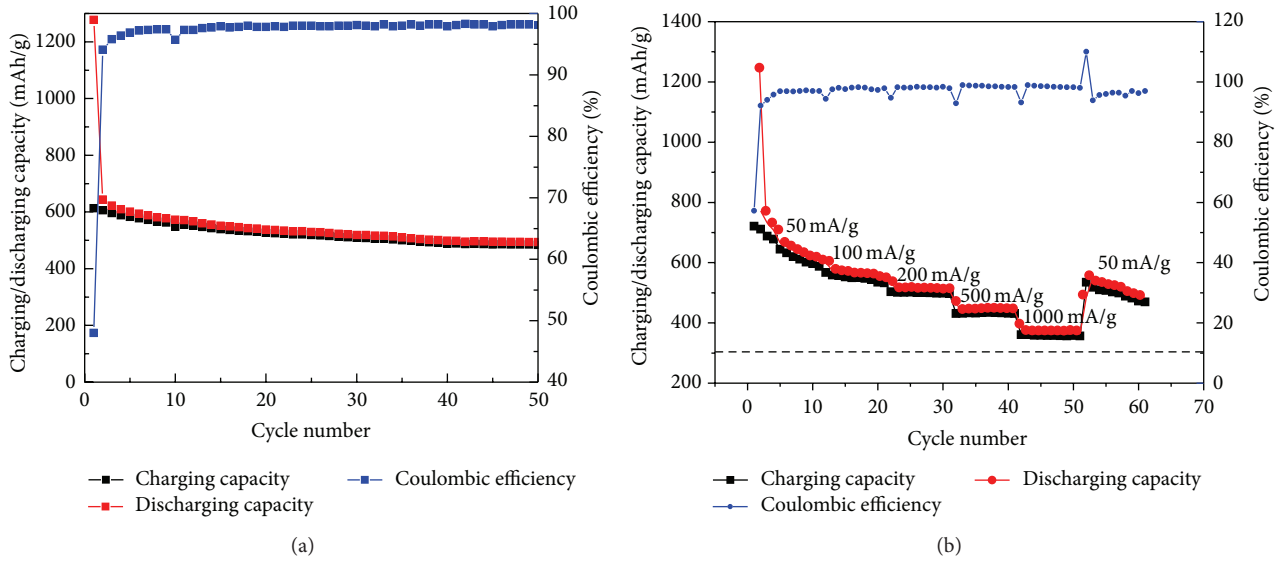

FIGURE 4: (a) Cyclic performance and Coulombic efficiency of the SnS/SnS_2 nanoflower at a current density of 100 mAg^{-1} for 50 cycles. (b) Rate performance of the SnS/SnS_2 nanoflower at different current densities (50 mA/g, 100 mA/g, 200 mA/g, 500 mA/g, 1000 mA/g, and 50 mA/g).

corresponding to an initial Coulombic efficiency of 48%. Attributed to the possible irreversible processes, such as electrolyte decomposition and formation of SEI layer, the large volume changing, during the lithiation/delithiation process, often causes a drastic pulverization problem [17]. It is an effective method to produce a nanometer-sized frame, which cannot only shorten the pathway lengths of lithium-ions but also compensate the volume change due to their large surface-to-volume ratio, by morphology controlling [18]. After the first discharge, the discharge-charge profiles become stable. The second discharge capacity was found to be 643 $mAhg^{-1}$, which is 81.4% of the maximum theoretical reversible capacity of pure SnS (790 $mAhg^{-1}$). During the following cycles, the discharge capacity and charge capacity are kept well and the Coulombic efficiency is on the increase and reaches up to 98%, suggesting excellent capacity retention of the flower-like SnS/SnS_2 hierarchitecture. A high charge capacity of about 500 $mAhg^{-1}$ is attained after 50 cycles.

Figure 4(b) shows the rate performance of the SnS/SnS_2 nanoflower, with the current density changing from 50 to 1000 mA/g and returning to 50 mA/g in the voltage range of 0.02 to 1.3 V. In spite of the cycling at high current density, the discharge capacity recovered to 486 mAh/g, when the current density returned to 50 mA/g. This is the powerful evidence to indicate the excellent rate performance of this nanostructure.

4. Conclusions

In summary, the three-dimensional flower-like hierarchitectures constructed by SnS/SnS_2 heterostructures nanosheets have been synthesized using a simple one-pot hydrothermal method. The as-synthesized products exhibit a highly reversible lithium storage performance as an anode material of lithium-ion batteries with exhibiting high charge/discharge capacity and excellent reversibility over 50 cycles. These novel SnS/SnS_2 heterostructures would be one of the most potential nanostructures in energy and nanodevices in the future.

Conflict of Interests

The authors declare that there is no conflict of interests regarding the publication of this paper.

Acknowledgments

This work is supported by a fund from the National Natural Science Foundation of China (Grant no. 11004089) and the Fundamental Research Funds for the Central Universities, nos. lzujbky-2013-185 and lzujbky-2014-38.

References

[1] Y. C. Liu, H. Y. Kang, L. F. Jiao et al., "Exfoliated-SnS_2 restacked on graphene as a high-capacity, high-rate, and long-cycle life anode for sodium ion batteries," *Nanoscale*, vol. 7, no. 4, pp. 1325–1332, 2015.

[2] X. G. Han, X. Han, L. Q. Sun et al., "One-step synthesis of highly aligned SnO_2 nanorods on a self-produced $Na_2Sn(OH)_6$ substrate for high-performance lithium-ion batteries," *CrystEngComm*, vol. 17, no. 8, pp. 1754–1757, 2015.

[3] K. J. Koski and Y. Cui, "The new skinny in two-dimensional nanomaterials," *ACS Nano*, vol. 7, no. 5, pp. 3739–3743, 2013.

[4] J.-G. Kang, Y.-D. Ko, K. J. Choi, J.-G. Park, and D.-W. Kim, "Fabrication of tin monosulfide nanosheet arrays using laser ablation," *Applied Physics A*, vol. 103, no. 2, pp. 505–510, 2011.

[5] Y. J. Zhang, J. Lu, S. L. Shen, H. R. Xu, and Q. B. Wang, "Ultralarge single crystal SnS rectangular nanosheets," *Chemical Communications*, vol. 47, no. 18, pp. 5226–5228, 2011.

[6] Y. Y. Mai and A. Eisenberg, "Self-assembly of block copolymers," *Chemical Society Reviews*, vol. 41, no. 18, pp. 5969–5985, 2012.

[7] P. Sun, W. Zhao, Y. Cao, Y. Guan, Y. Sun, and G. Lu, "Porous SnO_2 hierarchical nanosheets: hydrothermal preparation, growth mechanism, and gas sensing properties," *CrystEngComm*, vol. 13, no. 11, pp. 3718–3724, 2011.

[8] L. Zhang, Y. N. Guo, J. Peng et al., "3-D flowerlike architectures constructed by ultrathin perpendicularly aligned mesoporous nanoflakes for enhanced asymmetric catalysis," *Chemical Communications*, vol. 47, no. 14, pp. 4087–4089, 2011.

[9] D. D. Vaughn II, O. D. Hentz, S. R. Chen, D. H. Wang, and R. E. Schaak, "Formation of SnS nanoflowers for lithium ion batteries," *Chemical Communications*, vol. 48, no. 45, pp. 5608–5610, 2012.

[10] C. Julien and C. P. Vicente, "Vibrational studies of lithium-intercalated SnS_2," *Solid State Ionics*, vol. 89, no. 3-4, pp. 337–343, 1996.

[11] S. Sohila, M. Rajalakshmi, C. Ghosh, A. K. Arora, and C. Muthamizhchelvan, "Optical and Raman scattering studies on SnS nanoparticles," *Journal of Alloys and Compounds*, vol. 509, no. 19, pp. 5843–5847, 2011.

[12] C. Xu, Y. Zeng, X. H. Rui et al., "Controlled soft-template synthesis of ultrathin C@FeS nanosheets with high-Li-storage performance," *ACS Nano*, vol. 6, no. 6, pp. 4713–4721, 2012.

[13] Y. T. Zhong, X. Wang, K. C. Jiang et al., "A facile synthesis and lithium storage properties of Co_3O_4-C hybrid core-shell and hollow spheres," *Journal of Materials Chemistry*, vol. 21, no. 44, pp. 17998–18002, 2011.

[14] X. Jiang, X. L. Yang, Y. H. Zhu, J. H. Shen, K. C. Fan, and C. Z. Li, "In situ assembly of graphene sheets-supported SnS_2 nanoplates into 3D macroporous aerogels for high-performance lithium ion batteries," *Journal of Power Sources*, vol. 237, pp. 178–186, 2013.

[15] C. X. Zhai, N. Du, and H. Z. D. Yang, "Large-scale synthesis of ultrathin hexagonal tin disulfide nanosheets with highly reversible lithium storage," *Chemical Communications*, vol. 47, no. 4, pp. 1270–1272, 2011.

[16] J. Xia, G. Li, Y. Mao, Y. Li, P. Shen, and L. Chen, "Hydrothermal growth of SnS_2 hollow spheres and their electrochemical properties," *CrystEngComm*, vol. 14, no. 13, pp. 4279–4283, 2012.

[17] S. Liu, X. M. Yin, L. B. Chen, Q. H. Li, and T. H. Wang, "Synthesis of self-assembled 3D flowerlike SnS_2 nanostructures with enhanced lithium ion storage property," *Solid State Sciences*, vol. 12, no. 5, pp. 712–718, 2010.

[18] Y. P. Du, Z. Y. Yin, X. H. Rui et al., "A facile, relative green, and inexpensive synthetic approach toward large-scale production of SnS_2 nanoplates for high-performance lithium-ion batteries," *Nanoscale*, vol. 5, no. 4, pp. 1456–1459, 2013.